The Parametric Differential Method: An Alternative to the Calculation of Form Factors

Gladimir V. Guimarães Baranoski

Informatics Institute - CPGCC - UFRGS - Caixa Postal 15064 - Porto Alegre - Brasil
FAX: (051) 336-5576 - E-mail: gladimir@inf.ufrgs.br

Abstract

The parametric differential method calculates the form factors without using approximations by polygons. Because of this it contributes to the improvement of the realism of the images synthesised through the radiosity method. This paper presents the most important characteristics of the parametric differential method as well as the results concerning its accuracy. Comparison of the form factors found using the new algorithm has been made with those analytically found.

Keywords: form factor, radiosity, image synthesis.

1. Introduction

The parametric differential method, and henceforth referred to as the PDM, has as its main aim to allow the application of the radiosity method to the image synthesis of objects formed by curved surfaces without achieving approximations by polygons. This is its main characteristic and no such algorithm has been reported in the literature to date.

The PDM computes the form factors between surfaces taking into account their parametric descriptions. The surfaces are divided into patches in order to increase the accuracy of the form factors and to provide more accurate radiosities for sectors of the surfaces. Regarding curved surfaces, the division into curved patches, instead of polygons, allows a more accurate representation.

The calculation of form factors between finite surfaces involves the resolution of double area integrals. The PDM, like other methods of form factors calculation, solve these integrals using a numerical integration method. The main difference between the PDM and the usual methods resides in the transformation of the mathematical expression of the form factors in order to make it more general.

Its terms are expressed in a vector form and take into account the parametric variables used to describe the surfaces. The integrals are evaluated along the limits of the parametric variables without performing approximations of curved contours through the use of line segments.

In addition, the occlusion testing performed by PDM includes curvature tests which consider the vector characteristics of the calculation of the form factors. These tests influence directly the accuracy of the results and allow a reduction of the number of operations executed during the evaluation of the form factors.

2. Fundamental Concepts

2.1. Expression of the Parametric Area Differential

Using the concepts of the vector field theory [1], suppose that a surface S, described in a three dimensional space, R^3 , can be parametrized by a continuously differentiable function g(t,s):

$$R^2 \overset{g}{\Longrightarrow} R^3 \tag{1}$$

The function g(t,s) can be written in the following form:

$$g(t,s) = \begin{bmatrix} x = g_1(t,s) \\ y = g_2(t,s) \\ z = g_3(t,s) \end{bmatrix} \tag{2}$$

where the parameters **t** and **s** belong to some set D in R^2 .

It is known that at each point g(t,s) in S the tangent vectors are defined through vector partial derivatives:

$$\frac{\partial g(t,s)}{\partial t} \quad and \quad \frac{\partial g(t,s)}{\partial s} \tag{3}$$

and these vectors are linearly independent.

Then the normal vector at a point g(t,s) on a surface S can be expressed by the cross product of the tangent vectors:

$$\vec{n}(t,s) = \frac{\partial g(t,s)}{\partial t} \times \frac{\partial g(t,s)}{\partial s} \tag{4}$$

The area of the surface S is usually calculated through the integration over S of an area differential, composed by cartesian variables:

$$Area\ of\ S = \int_s dA \tag{5}$$

However, the area of S can also be determined through the integration along D of an area differential, composed by the parametric variables **t** and **s**. From analytical geometry it is known that the length of the cross product between two vectors $\vec{a}$ and $\vec{b}$ corresponds to the area of the parallelogram formed by $\vec{a}$ and $\vec{b}$. Applying this concept to the expression (4) leads to the following equation:

$$|\vec{n}| = \left| \frac{\partial g(t,s)}{\partial t} \times \frac{\partial g(t,s)}{\partial s} \right| \tag{6}$$

Thus, if $|\vec{n}\ |$ is obtained at the points $g(t_k, s_k)$ corresponding to nodes (t_k, s_k) of a grid over D, the area of S can be expressed as:

$$Area\ of\ S = \int_D |\vec{n}|\ \ d_s d_t \tag{7}$$

Comparing the expression (7) with the expression (5) and using the limits of the parametric variables **t** and **s** in D as integration limits, the following expression for the parametric area differential results:

$$dA_{parametric} = |\vec{n}|\ \ d_s d_t \tag{8}$$

Another way to explain the equation above is using the concept of *jacobian determinant* of the mapping from D to R^3 [2].

2.2. Form Factor between two Finite Parametric Surfaces

The expression of the form factor between two finite surfaces, A_1 and A_2, is given by:

$$F_{1-2} = \frac{1}{A_1} \int_{A_1} \int_{A_2} \frac{\cos\alpha_1 \ \cos\alpha_2}{\pi L^2} \, dA_2 \, dA_1 \tag{9}$$

Taking into account that the two surfaces are described by parametric variables, the form factor F_{1-2} is calculated using the geometry sketched in Figure 1.

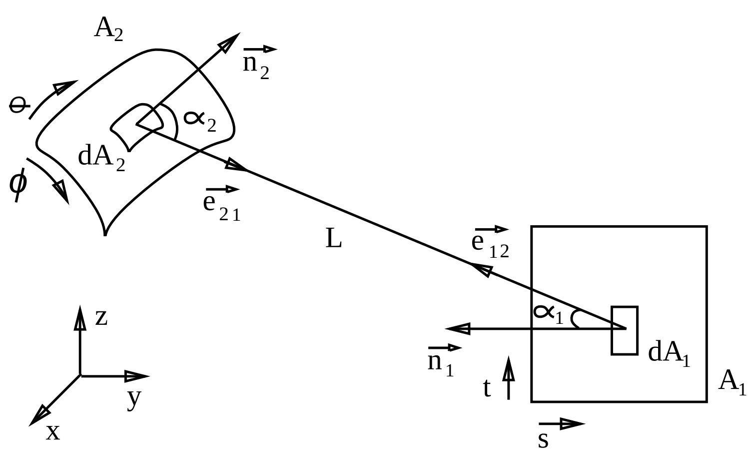

t,s	=	parametric variables that describe the surface A_1.
θ, ϕ	=	parametric variables that describe the surface A_2.
$\vec{n}_1$	=	normal vector to surface A_1 in a point $P_1(t, s)$.
$\vec{n}_2$	=	normal vector to surface A_2 in a point $P_2(\theta, \phi)$.
$\vec{e}_{12}$	=	visibility vector from P_1 to P_2.
$\vec{e}_{21}$	=	visibility vector from P_2 to P_1.
α_1	=	angle between $\vec{n}_1$ and $\vec{e}_{12}$.
α_2	=	angle between $\vec{n}_2$ and $\vec{e}_{21}$.
L	=	distance between P_1 and P_2.

Figure 1: Geometry of the form factor between two finite parametric surfaces.

From analytical geometry it is known that the cosine of an angle α between two vectors $\vec{a}$ and $\vec{b}$ is given by the dot product of these vectors. Thus, the cosines of α_1 and α_2 are given by:

$$\cos\alpha_1 = \frac{\vec{n}_1 \ . \ \vec{e}_{12}}{|\vec{n}_1| \ |\vec{e}_{12}|} \quad and \quad \cos\alpha_2 = \frac{\vec{n}_2 \ . \ \vec{e}_{21}}{|\vec{n}_2| \ |\vec{e}_{21}|} \tag{10}$$

The expression (8) leads to the following expressions for the area differentials dA_1 and dA_2:

$$dA_1 = |\vec{n}_1| \ d_s d_t \quad and \quad dA_2 = |\vec{n}_2| \ d_\phi d_\theta \tag{11}$$

Similarly, using the expression (7), the following equations for the areas A_1 and A_2 are obtained:

$$A_1 = \int_t \int_s |\vec{n}_1| \ d_s d_t \quad and \quad A_2 = \int_\theta \int_\phi |\vec{n}_2| \ d_\phi d_\theta \tag{12}$$

After replacing the expressions (10) to (12) into expression (9) and expressing the integration between the limits of the parametric variables, the equation of the form factor becomes:

$$F_{1-2} = \frac{1}{\int_t \int_s |\vec{n}_1| \; d_s d_t} \int_\theta \int_\phi \int_t \int_s \frac{(\vec{n}_1.\vec{e}_{12})\,(\vec{n}_2.\vec{e}_{21})\,|\vec{n}_1|\,|\vec{n}_2|}{|\vec{n}_1|\,|\vec{e}_{12}|\,|\vec{n}_2|\,|\vec{e}_{21}|\,\pi L^2} \; d_s d_t d_\phi d_\theta \tag{13}$$

It is known that the distance L corresponds to the module of the vector $\vec{e}_{12}$, which has the same value of the module of the vector $\vec{e}_{21}$:

$$L = |\vec{e}_{12}| = |\vec{e}_{21}| \tag{14}$$

Thus, after performing the substitutions and simplifications in the equation (13), the equation that defines the form factor between two finite parametric surfaces is expressed as:

$$F_{1-2} = \frac{1}{\pi \int_t \int_s |\vec{n}_1| \; d_s d_t} \int_\theta \int_\phi \int_t \int_s \frac{(\vec{n}_1.\vec{e}_{12})\,(\vec{n}_2.\vec{e}_{21})}{L^4} \; d_s d_t d_\phi d_\theta \tag{15}$$

In order to calculate the numerical value of F_{1-2}, the latter expression is evaluated using the numerical integration method known as Gaussian quadrature [3-4]. This method consists, basically, of solving the integrals by changing them into summations. Considering the surfaces are divided into patches, the summation corresponding to the form factor between two patches **a** and **b** is given by:

$$F_{a-b} = \frac{1}{A_a} \sum_{i=1}^{p} \sum_{j=1}^{p} \sum_{k=1}^{p} \sum_{r=1}^{p} w_i w_j w_k w_r \; \mathbf{f}\left(s_i, t_j, \phi_k, \theta_r\right) \tag{16}$$

where:

A_a	$=$ area of patch **a**.
$\mathbf{f}\left(s_i, t_j, \phi_k, \theta_r\right)$	$= \frac{(\vec{n}_a.\vec{e}_{ab})\,(\vec{n}_b.\vec{e}_{ba})}{|\vec{e}_{ab}|^4}$
w_i, w_j, w_k, w_r	$=$ Gaussian weight coefficients.
p	$=$ number of Gaussian points.

The function **f** is evaluated applying the vectors $\vec{n}$ and $\vec{e}$ at sample points distributed over the patches. The coordinates of these sample points are given through the parametric equations that describe the surfaces. The number of evaluations of the function **f**, *i.e.* the number of the terms of the summation, corresponds to p^4 and the number of sample points for each patch corresponds to p^2.

3. Occlusion Testing

The parametric differential method allows the calculation of form factors between two surfaces. If there is an obstacle between them some points of a surface are not visible from points of the other. In this case, as the numerical integration corresponding to the form factors equation consists in the evaluation of a summation, the terms of this summation that correspond to the points of a surface not visible from points of another surface have not to be computed. This procedure is directly associated with the accuracy of PDM and avoids the execution of unnecessary calculations.

The approach used to determine occlusion is similar to the ray-tracing technique used by Wallace *et al.* [5]. Instead of shooting rays from the vertices of polygons as the latter technique does, lines are used to connect sample points of a patch to sample points of another patch. These sample points are the same as those used in the numerical evaluation of the expression (16).

The occlusion testing is essentially the verification of whether or not there is an intersection between a line L, which connects two sample points P_a and P_b, and an obstacle between the patches. If there is an intersection, the sample point P_a of the patch **a** is not visible from the sample point P_b of the patch **b** and vice-versa. In this case, the term corresponding to the pair P_aP_b must not be added to the summation concerning the form factor between the patch **a** and the patch **b**. This means that the function **f**(t,s,ϕ,θ) (expression (16)) is not evaluated to the pair of sample points P_a and P_b.

Even if there is no intersection with the obstacle the term corresponding to P_a and P_b may be discarded due to the possibility of curvature of one or both patches. In this case another test should be applied to verify the visibility condition between the points P_a and P_b. Since these tests are associated with the curvature, the technique is called curvature testing.

3.1. Curvature Testing between a Curved Surface and a Plane Surface

Consider a plane surface A_1 and a curved surface A_2. In order to obtain the form factor F_{1-2} the points of A_2 that are not visible by the points of A_1 should be discarded.

The curvature testing between two points P_1 and P_2, that belong to the surfaces A_1 and A_2 respectively, consists of the dot product of the vectors $\vec{n}_2$ and $\vec{e}_{21}$. The vector $\vec{n}_2$ corresponds to the normal at a point P_2 of the surface A_2. The vector $\vec{e}_{21}$ corresponds to the visibility vector from the point P_2 to the point P_1. The coordinates of the points P_1 and P_2, which are used in the expression of $\vec{n}$ and $\vec{e}$, are given through the parametric equations which describe the surfaces considering the limits of the parametric variables and the number of Gaussian points used in the numerical evaluation of the integrals.

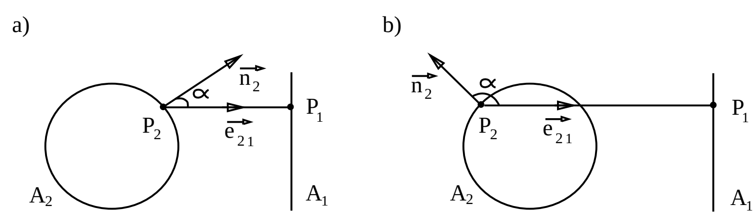

Figure 2: Visibility of a point of the surface A_2 from a point of the surface A_1: a) visible b) not visible.

If the dot product is positive it means that the angle α between the two vectors is in the range of 0^0 to 90^0, and the point P_2 is visible from the point P_1 (Figure 2a). Otherwise, if the dot product is negative, it means that the angle α between the two vectors is in the range of 90^0 to 180^0, and the point P_2 is not visible from the point P_1 (Figure 2b). In the first case the term of the summation corresponding to P_1P_2 must be evaluated. In the second case it must not be evaluated.

The tests shall be accomplished considering the visibility of the points of the curved surface A_2 from the points of the plane surface A_1. If just one dot product is used to determine the visibility the dot product at the point which belongs to the curved surface shall be calculated. Figure 3 illustrates a situation where the dot product is calculated at the point that belongs to the plane surface. In this case the dot product between $\vec{n}_1$ and $\vec{e}_{12}$ is positive and the angle α is in the range of 0^0 and 90^0 , but P_1 is not visible from P_2.

In order to obtain the form factor F_{2-1}, from the curved surface to the plane surface, F_{1-2} is calculated first. Then, using the reciprocity relationship of the form factors [6], F_{2-1} is determined.

Another way to determine visibility between the points P_1 and P_2 in Figure 3, independently of the direction of visibility, is to perform the calculation of the two dot products, regarding P_1 and P_2. If both dot products are calculated there is no possibility of mistake. This approach is used in the curvature testing between two curved surfaces which is presented afterwards.

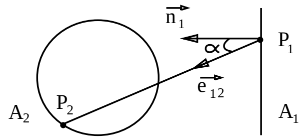

Figure 3: Incorrect application of the curvature testing.

3.2. Curvature Testing between two Curved Surfaces

Consider A_1 and A_2 as two curved surfaces. In this situation it is necessary to calculate two dot products at the points P_1 and P_2 which belong to the surfaces A_1 and A_2 respectively. The visibility situations corresponding to this situation are sketched in Figure 4. If both dot products are positive the points are mutually visible (Figure 4a). If one dot product is negative the angle α is greater than 90^0 and the points are not visible to each other (Figure 4b). The same conclusion is valid in the case of the two dot products being negative (Figure 4c).

The calculation of the two dot products has the aim of avoiding the incorrect determination of the visibility between two points, which can happen if only one observation direction is taken. For instance, in the situation described in Figure 4b, if only the dot product concerning the angle α_1 were calculated the point P_2 would be considered visible from the point P_1, which would undoubtedly be incorrect.

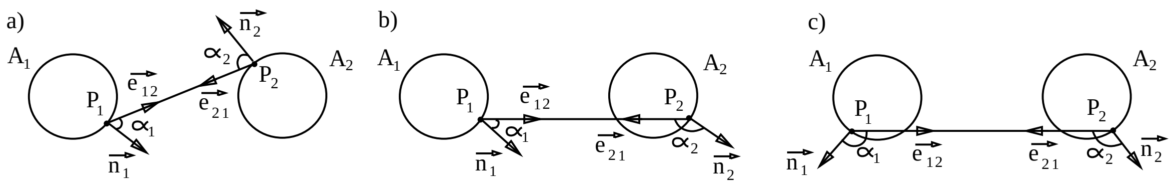

Figure 4: Visibility situations between two curved surfaces.

3.3. Curvature Testing on Concave Surfaces

The algorithms described in this paper can be applied to convex or concave surfaces. Figure 5 illustrates the curvature testing applied to a concave and a plane surface. The curvature testing can also be applied to two concave surfaces.

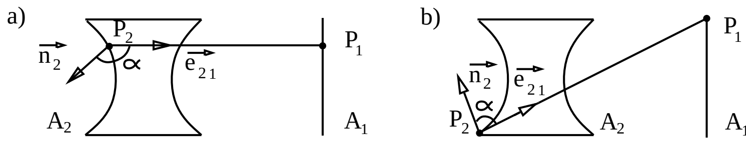

Figure 5: Curvature testing on a concave surface: a) $\vec{n}_2 \,.\, \vec{e}_{21} < 0$ b) $\vec{n}_2 \,.\, \vec{e}_{21} > 0$.

However, in the case of the concave surfaces, testing for self intersection may be also necessary. If the dot product is negative the point P_2 is not visible from P_1 (Figure 5a). On the other hand, if the dot product is positive testing for self intersection is necessary to decide about the visibility of P_2 from P_1. For instance, as in Figure 5b, the dot product at P_2 is positive but P_2 cannot be seen from P_1, because the same surface which P_2 is on, obscures it.

In addition, a concave surface can see itself ($F_{ii} \neq 0$)[6]. Consequently the solution for the series of equations that provides the radiosities of the environment will require the use of a pivot strategy [3-4] before the use of a standard equation solver.

4. Verification of the Accuracy of the Form Factors

The first images synthesised through the application of the radiosity method [6] have used an environment formed by the faces of a cube as a test model. The test model used in this paper adds a sphere to the model used by Goral *et al.* [6], since the development of PDM is particularly associated to the image synthesis of curved objects [7].

This simple test model, shown in Figure 6, was chosen because it supports, completely, the goals of this paper. It is composed of a curved object interacting, through the light interreflections, with the walls or faces of a surrounding cube. The sphere is an obstacle which allows the application of the occlusion testing technique described earlier.

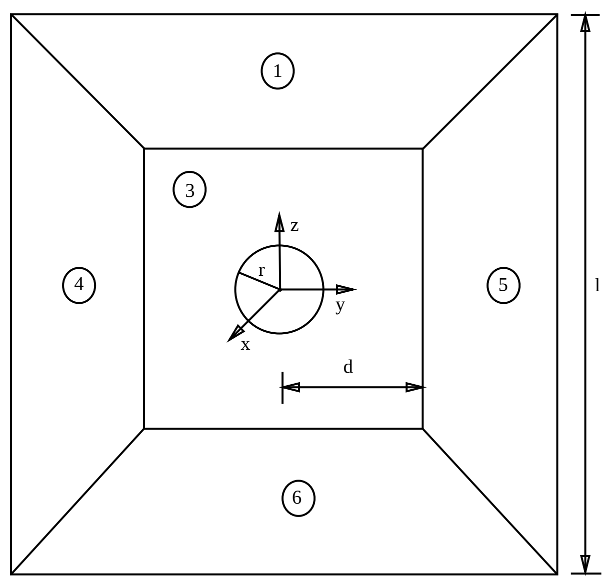

Face 2 is frontal.

r = sphere radius.
l = length of the faces of the cube.
d = distance between the sphere and the faces.

Figure 6: Sketch of the test model.

Additionally, the analytical form factors between the sphere and the walls, used in the determination of the relative errors corresponding to the form factors calculated by the PDM, are given by the form factor definition itself. Through the c summation relationship of the form factors [6], it is known that the summation of the form factors of a surface regarding the other surfaces that compose the closed environment is equal to 1. Therefore, the form factor between the sphere and each face of the cube, F_{s-f}, corresponds to 1/6, since the cube has six faces and the form factor of the sphere related to itself is zero.

$$F_{s-f(analytical)} = \frac{1}{6} = 1.6666 \times 10^{-1} \quad \text{to} \quad \text{f} = 1, 2, 3, 4, 5, 6 \tag{17}$$

The relative errors of the numerical form factors are calculated using the following expression presented by Maxwell *et al.* [8]:

$$Relative\ \ Error(\%) = \frac{|analytical\ \ value - numerical\ \ value|}{analytical\ \ value} \times 100 \tag{18}$$

The parametric equations of the sphere used in this paper correspond to the geometry described in Figure 7a and are expressed as:

$$g_e(\phi, \theta) = \begin{bmatrix} x(\phi, \theta) = r\ \sin\phi\ \cos\theta \\ y(\phi, \theta) = r\ \sin\phi\ \sin\theta \\ z(\phi, \theta) = r\ \cos\phi \end{bmatrix} \tag{19}$$

The normal to the sphere surface can be obtained through the following cross product:

$$\vec{n}_e = \frac{\partial g_e(\phi, \theta)}{\partial \phi} \times \frac{\partial g_e(\phi, \theta)}{\partial \theta} \tag{20}$$

Using the equations presented in (19) and (20), the normal to the sphere is given by:

$$\vec{n}_e = (r^2 \sin^2\phi \cos\theta, r^2 \sin^2\phi \sin\theta, r^2 \cos\phi \sin\phi) \tag{21}$$

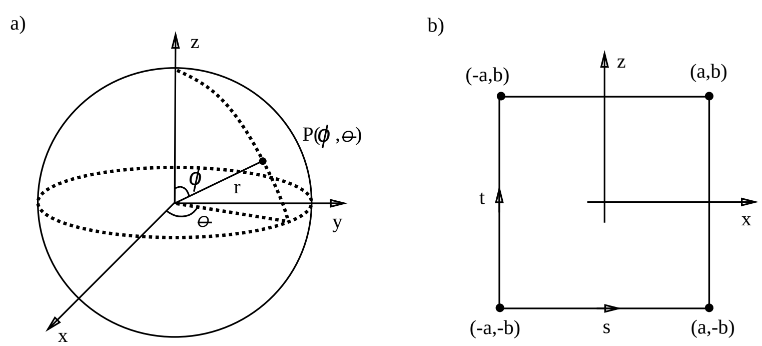

Figure 7: Geometries used in the parametric descriptions of: a) the sphere b) a plane patch.

The parametric equations used to describe the plane patches in this paper correspond to the geometry presented in Figure 7b and are expressed as:

$$g_p(t, s) = \begin{bmatrix} x(t, s) = a(2s - 1) \\ y(t, s) = d \\ z(t, s) = b(2t - 1) \end{bmatrix} \tag{22}$$

where a and b are the coordinates of the vertices of a plane patch.

The normal to the plane patches can also be obtained through the cross product of the partial derivates of g_p(t,s):

$$\vec{n}_p = \frac{\partial g_p(t,s)}{\partial t} \times \frac{\partial g_p(t,s)}{\partial s} \tag{23}$$

Thus, to a plane patch with a geometry described in Figure 7b, the normal vector is given by:

$$\vec{n}_p = (0, l^2, 0) \tag{24}$$

4.1 Form Factors between the Sphere and the Faces

The values assigned to the parameters **r**, **d** and **l** were 1, 3 and 6 respectively. The closed environment was divided into 86 patches, 32 for the sphere and 9 patches for each face. The form factors between the patches of the sphere and the patches of the faces were calculated. Then, the form factors between the sphere and each face were also calculated to determine the relative errors. The expression for these form factors was obtained from the expression used in the substructuring technique [9] and is given by:

$$F_{s-f} = \frac{1}{A_s} \sum_{pf=1}^{n_{pf}} \sum_{ps=1}^{n_{ps}} F_{ps-pf}\ A_{ps} \tag{25}$$

where:
F_{s-f} = form factor between the sphere and a face.
F_{ps-pf} = form factor between a patch of the sphere and a patch of a face.
A_s = area of the sphere.
A_{ps} = area of the patches of the sphere.
n_{pf} = number of patches of the face.
n_{ps} = number of patches of the sphere.

The values of the relative errors will be lower if the sphere and the faces are divided into a finer grid of patches. In order to demonstrate this assumption, the environment was also divided into 280 patches, 64 for the sphere and 36 for each face. The form factors obtained, using the five Gaussian points, are listed in Table 1.

Table 1: Form factors between the sphere and the faces.

Face	86 patches		280 patches	
	F$_{s-f(numerical)}$	Relative Error(%)	F$_{s-f(numerical)}$	Relative Error(%)
1	1.6735×10^{-1}	0.41	1.6683×10^{-1}	0.10
2	1.6693×10^{-1}	0.16	1.6673×10^{-1}	0.04
3	1.6693×10^{-1}	0.16	1.6673×10^{-1}	0.04
4	1.6693×10^{-1}	0.16	1.6673×10^{-1}	0.04
5	1.6693×10^{-1}	0.16	1.6673×10^{-1}	0.04
6	1.6735×10^{-1}	0.41	1.6683×10^{-1}	0.10

Even though there is a small variation concerning the form factors of the faces 1 and 6 due to the characteristics of the parametric equations used in the description of the surfaces, the presented accuracy is excellent. The calculation was performed on a SUN Sparc station 1+. The processing times corresponding to each subdivision of the environment are listed in Table 2.

Table 2: Processing times of the form factors between the sphere and the faces.

No. of Patches	Processing Time
86	36sec
280	5min

4.2 Form Factors between the Faces

A problem of indetermination appears when two sample points, which belong to two different patches, are placed almost at the same point on the edge shared by these patches. The distance **L** between the sample points may be too small due to the Gaussian distribution of the sample points. Then, the numerator and the denominator of the function **f**(s,t,ϕ,θ) will have values close to zero. In order to solve this problem the rules of L'Hopital [10] must be applied to the numerator and to the denominator of the function **f**(t,s,ϕ,θ). A new function **f'**(t,s,ϕ,θ) is obtained. This function should be used during the evaluation of the summation terms (16) regarding the pairs of sample points with a geometry described earlier.

The form factors between the patches of the faces were calculated performing the correction described above. In order to verify the consistency and the accuracy of the obtained values the form factors between the faces were determined using the following equation, which also comes from the expression presented by Cohen *et al.* [9]:

$$F_{fa-fb} = \frac{A_{pa}}{A_a} \sum_{pb=1}^{n_{pb}} \sum_{pa=1}^{n_{pa}} F_{pa-pb} \tag{26}$$

where:
F_{fa-fb} = form factor between the face **a** and the face **b**.
F_{pa-pb} = form factor between a patch of the face **a** and a patch of the face **b**.
A_a = area of the face **a**.
A_{pa} = area of a patch of the face **a**.
n_{pa} = number of patches of the face **a**.
n_{pb} = number of patches of the face **b**.

As was performed in the previous section, the form factors of the faces were calculated twice, considering the closed environment divided into 86 patches and 280 patches. The form factors obtained, using five Gauss points in the numerical evaluation of integrals, are presented in Table 3. They are consistent with the geometry of the environment (Figure 7). As expected, the pairs of faces with the same geometric positions, parallel or perpendicular, have the same form factor values.

The summation relationship of the form factors can be used to evaluate the accuracy of the form factors obtained. As was mentioned earlier the form factors for each surface of a closed environment must sum to unity. Face 1 was chosen as an example. Its form factors regarding the sphere were obtained from the values presented in section 4.1 and using the reciprocity relationship of the form factors [6]. The form factors between face 1 and the other faces are presented in Table 3.

The values of the summations of the form factors of face 1 concerning the other surfaces, considering the environment divided into 86 and 280 patches, are presented in Table 4. These values present a very satisfactory degree of accuracy, even though future research still needs to be done to improve the technique used to solve the problem of indetermination mentioned earlier. A radiosity program which implements the hemi-cube method [13] has not yet been written to compare the two algorithms, however, let us just recall that Baum *et al.* [11] mention relative errors of 2.5% for the form factors obtained through the hemi-cube method.

The increase in the number of patches improved the accuracy as well as increased the processing time required. The evaluation of the form factors between the faces was also performed on a SUN Sparc station 1+. The processing times, considering both subdivisions of the environment, are listed in Table 5.

Table 3: Form factors between the faces.

face$_a - face_b$	$F_{fa-fb(numerical)}$	
	86 patches	280 patches
1-2	2.0341×10^{-1}	2.0018×10^{-1}
1-3	2.0341×10^{-1}	2.0018×10^{-1}
1-4	2.0341×10^{-1}	2.0018×10^{-1}
1-5	2.0341×10^{-1}	2.0018×10^{-1}
1-6	1.5400×10^{-1}	1.5400×10^{-1}
2-3	1.5400×10^{-1}	1.5400×10^{-1}
2-4	2.0341×10^{-1}	2.0018×10^{-1}
2-5	2.0341×10^{-1}	2.0018×10^{-1}
2-6	2.0341×10^{-1}	2.0018×10^{-1}
3-4	2.0341×10^{-1}	2.0018×10^{-1}
3-5	2.0341×10^{-1}	2.0018×10^{-1}
3-6	2.0341×10^{-1}	2.0018×10^{-1}
4-5	1.5400×10^{-1}	1.5400×10^{-1}
4-6	2.0341×10^{-1}	2.0018×10^{-1}
5-6	2.0341×10^{-1}	2.0018×10^{-1}

Table 4: Summations of the form factors between face 1 and the other surfaces.

No. of Patches	Summation	Relative Error(%)
86	1.0258	2.58
280	1.0128	1.28

Table 5: Processing times of the form factors between the faces.

No. of Patches	Processing Time
86	1min 22sec
280	21min 18sec

5. Conclusion

The PDM is an effective method for the calculation of form factors between plane and/or curved surfaces, whose main focus of attention is the numerical accuracy of the results. The fact that PDM does not use approximations by polygons represents an advantage over other methods of form factor calculation.

The form factors obtained from the use of this method present a high degree of accuracy. If the surfaces are divided into a finer grid of patches there is an increase of the accuracy. Certainly this increase in accuracy is followed by an increase in the processing time, which can be reduced through the application of parallelism on the calculations. Besides, with respect to curved surfaces, a larger number of polygons is necessary, instead of curved patches, to represent them without a significant decrease of realism. Since the number of operations executed during the calculation of form factors depends on the discretization of the surfaces, curved patches as as used by PDM, instead of polygons, allows a reduction of the processing time.

Beyond the accuracy of the form factors PDM benefits the use of the exact descriptions of the surfaces during the rendering, *i.e.* the curved surfaces are not divided in polygons. This avoids the polygonized silhouettes of the curved surfaces common in radiosity pictures. As we can see in Figure 8 the curved object does not present a contour formed by edges of polygons. This image was generated considering the diffuse environment sketched in Figure 6 divided in 280 patches and 144 subpatches corresponding to shadow area. It was rendered using a visible-surface ray casting algorithm [12] and no anti-aliasing technique was applied.

Despite the simple geometries used in the tests, we believe the PDM represents a step forward towards the search of accuracy in the physically-based rendering. Future efforts will include the study of applications of PDM on the calculation of specular form factors and its use in conjunction with other methods, for example the ray-tracing technique presented by Wallace *et al.* [5], in order to generate complex images using a progressive refinement strategy. In addition, parallelism will be applied to the calculation of the form factors to reduce the processing time.

6. References

1. R.E.Willianson, R.H.Crowell and H.F.Totter, *Calculus of Vector Functions*, Prentice Hall, Englewood, Cliffs, 2nd edition, 1968.
2. J.G.Ergatoudis, *Isoparametric Finite Elements in Two and Three Dimensional Stress Analysis,* University College of Swansea, School of Engineering, 1968. (PhD Dissertation)
3. B.Carnahan, H.A.Luther and J.O.Wilker, *Applied Numerical Methods*, John Willey, 1969.
4. W.H. Press, B.P.Flannery, S.A.Teukolsky and W.T.Vetterling, *Numerical Recipes in C The Art of Scientific Computing*, Cambridge University Press, 1988.
5. J.R. Wallace, K.A.Elmquist and E.A.Haines, "A Ray Tracing Algorithm for Progressive Radiosity", Computer Graphics, **23**(3) pp. 315-325 (1989).
6. C.M.Goral, K.E.Torrance, D.P.Greenberg and B.Battaile, "Modeling the Interaction of Light Between Diffuse Surfaces", Computer Graphics, **18**(2) pp. 213-222 (1984).
7. G.V.G.Baranoski, "Application of Radiosity to the Image Synthesis of Objects Formed by Curved Surfaces", In: Proceedings of III Brazilian Symposium on Computer Graphics and Image Processing, pp. 11-20 (1990).
8. G.M.Maxwell, M.J.Bayley and V.M.Goldschimdt, "Calculation of the Radiation Configuration Factor Using Ray Casting", CAD, **18**(7) pp. 371-379 (1986).
9. M.F.Cohen, D.P.Greenberg, P.S.Immel, P.J.Brock. "An Efficient Radiosity Approach for Realistic Image Synthesis", IEEE Computer Graphics and Applications, **6**(3) pp. 26-35 (1986).
10. W.A.Granville, P.F.Smith and W.R.Longley, *Elements of the Differential and Integral Calculus*, Gim and Company, 1941.
11. D.R.Baum, H.E.Rushmeier and J.M.Winget, "Improving Radiosity Solutions through the Use of Analytically Determined Form Factors", Computer Graphics, **23**(3) pp. 325-334 (1989).
12. J.D.Foley, A.Van Dam, S.K.Feiner and J.F.Hughes, *Computer Graphics Principles and Practices*, Addison-Wesley, 2nd edition, 1990.
13. M.F.Cohen and D.P.Greenberg, "The Hemi-Cube: A Radiosity Solution for Complex Environments", Computer Graphics, **19**(3) pp. 31-40 (1985).

Acknowledgements

The author would like to thank Prof. Anatólio Laschuk for his support and help. The author is also grateful to his colleagues for the fruitful discussions, to the referees for their comments and suggestions and all those who helped in the preparation of this paper.